Tellus (2004), ??B, 1–6
Printed in UK. All rights reserved

TELLUS

Intercomparison between multi-angle imaging spectroradiometer and sunphotometer aerosol optical thickness in dust source regions over China: implications for satellite aerosol retrievals and radiative forcing calculations

By SUNDAR A. CHRISTOPHER* and JUN WANG, *Department of Atmospheric Sciences, University of Alabama in Huntsville, Huntsville, AL, USA*

(Manuscript received 3 February 2004; in final form 23 April 2004)

ABSTRACT

The multi-angle imaging spectroradiometer (MISR) aerosol optical thickness (AOT) product (τ_{MISR}) was compared with sunphotometer AOT (τ_{SP}) at Dunhuang (40.09°N, 94.41°E), located near the Takalamakan and Gobi dust source regions in China, during March–November 2000. This study is unique because AOT measurements from the ground are not routinely available at or near dust source regions. The τ_{MISR} and τ_{SP} are highly correlated, with linear correlation coefficients (R) ranging from 0.85 to 0.95 depending on the different comparison criteria used to assess the MISR retrievals. With one exception where τ_{MISR} shows large differences (>0.3) when compared with τ_{SP} during the passage of a dust front, all other collocated $\tau_{\mathrm{SP}}/\tau_{\mathrm{MISR}}$ pairs are highly correlated with $R > 0.9$ and with root-mean-square error of 0.06 when retrieval conditions are favourable. Overall, τ_{MISR} systemically over-estimate τ_{SP} by 0.05, but they all fall within the predicted uncertainties (0.05 or 20% of τ_{SP}, whichever is larger). Due to diurnal change of AOT, the difference between daily averaged τ_{SP} values and τ_{MISR} reported during MISR overpass time is about 0.09. We discuss the implications of these results for satellite aerosol retrievals and radiative forcing studies.

1. Introduction

The effect of aerosols on climate is one of the largest uncertainties in current global climate models (Hansen et al., 1997). Current understanding of the radiative forcing of dust aerosols is very limited (IPCC 2001), especially over dust source regions where ground observations are few and multispectral satellite retrievals at visible to near-infrared wavelengths are often difficult due to the high surface albedo (Kaufman et al., 2002). On the other hand, the multi-angle imaging spectroradiometer (MISR) routinely retrieves the aerosol optical thickness (AOT) at visible wavelengths over desert regions (Martonchik et al., 1998, 2002) and provides valuable information for the study of dust radiative forcing over bright targets (e.g. Zhang and Christopher, 2003).

Ground-based sunphotometer measurements (Holben et al., 2001) have been used extensively in the past for validation of satellite AOT retrievals (e.g. Remer et al., 2002) and to examine the uncertainties in the satellite retrieval algorithms (e.g. Wang et al., 2003a,b). Using ground-based and aircraft measurements, several experiments have been conducted to study the dust aerosol properties in the Saharan regions (e.g. Tanré et al., 2003). However, widely prevalent dust events ("yellow sand") from the Taklamakan and Gobi deserts in Northwest China, have only gained considerable attention recently (Husar et al., 2001). Using 10 months of AOT data collected near the Chinese dust source regions, we compare the sunphotometer AOT (τ_{SP}) with MISR AOT (τ_{MISR}) retrievals. We also discuss the implication of these results for the MISR AOT retrieval algorithms and radiative forcing studies.

2. Data

Ten months (March–November 2000) of AOT data inferred from a sunphotometer (model Pom-01, Prede Inc.) located at Dunhuang Airport (40.09°N, 94.41°E) were used in this study. The observation site is located at the eastern edge of the Takalamakan Desert, the southwestern edge of the Gobi Desert and the western edge of the Hexi Corridor in Gansu Province (Fig. 1). The sunphotometer measures the direct solar radiation centred at

*Corresponding author.
e-mail: sundar@nsstc.uah.edu

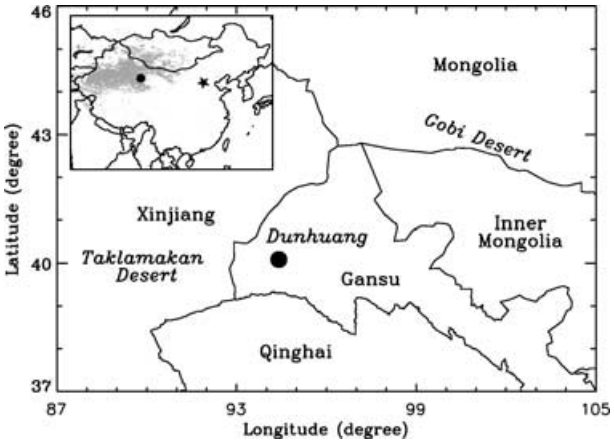

Fig 1. Map of the observation site Duhuang (denoted as filled circle) and its vicinity. The inset shows the map of Eastern Asia. The shaded area in the inset is the location of Taklamakan Desert and the Gobi Desert based on the on the USGS ecosystem database. The five-pointed star denotes the location of Beijing.

wavelengths of 315, 400, 500, 675, 870, 940 and 1020 nm and the AOT is calculated based on the Beer–Lambert–Bouguer law. The instrument has been carefully calibrated using a modified Langley plot approach (Nakajima et al., 1996) and included in the calculation is a correction for Rayleigh scattering, ozone optical depth based on Total Ozone Mapping Spectrometer (TOMS) level 3 data, and for variations in Earth–Sun distance. The random errors in calibration during each time step were filtered by using techniques outlined in Harrison and Michalsky (1994), and diurnal stability checks were performed according to the method outlined by Smirnov et al. (2000). Additionally, the measurements with the largest deviation (>0.02) from a second-order ln τ versus ln λ (λ is the wavelength) polynomial fit were rejected according to procedures outlined in Eck et al. (1999). A second-order polynomial fit between AOT and λ in logarithmic space gave excellent agreement with differences of the same order as the measurement uncertainty of AOT (approximately 0.01–0.02) (Eck et al., 1999). Manual cloud screening for questionable data was also performed with the help of weather observations obtained at the Dunhuang Meteorological Observatory. This data set is unique not only because the aerosol optical measurements in the Chinese dust source region are very sparse (Holben et al., 2001) but also because of its relatively long-term continuous observations.

The MISR level 2 AOT (τ_{MISR}) product (version F06_0013) on Terra has a spatial resolution of 17.6 × 17.6 km^2, and due to the narrow swath width of the sensor, global coverage can be obtained only every 7 to 9 d. The product contains AOT at 0.558 μm with an expected accuracy of 0.05 or 20%, whichever is larger (Kahn et al., 2001), and the algorithms and the associated products continue to evolve with time. The excellent agreement between τ_{MISR} and τ_{SP} has been reported for smoke aerosols over South Africa (Diner et al., 2001), but only a few comparisons have been made near dust source regions and no comparisons have been made in the dust source region near the Taklakaman Desert in East Asia. Since the sunphotometer does not have a channel at 0.558 μm, to compare the τ_{SP} with τ_{MISR}, we calculated τ_{SP} at 0.558 μm based on logarithmic interpolation between τ_{SP} at 0.5 μm and 0.675 μm.

3. Analysis and results

The sunphotometer (SP) continuously observes downward solar radiation with a 0.8° field of view of approximately for direct sun measurements at a fixed location, with a narrow wavelength interval of 0.01 μm (Holben et al., 2001). Compared with single-view-angle satellite sensors, the MISR is different because it images the same location from nine different angles at four different wavelengths and it takes about 7 min for all nine cameras to image a given location (Diner et al., 2001). In this study, we used the intercomparison procedure outlined in Diner et al. (2001) by selecting the τ_{SP} within 30 min of satellite overpass time and by comparing them with regional mean τ_{MISR} in 3 × 3 sets of 17.6 × 17.6 km^2 regions centred on the SP location. Using spatial quantities (mean and standard deviation) of satellite AOTs to compare with the temporal variations of SP measurements is a general approach to minimize the comparison errors (Zhao et al., 2002). It is important to note that beside the regional mean AOT, the MISR aerosol product also includes best-fit AOT and the regional-weighted AOT. The best-fit AOT is derived by fitting different type of aerosol mixtures to the MISR radiance observations and obtaining the minimum chi-squared fitting errors. However, the best-fit AOT is not necessarily a physically "successful" retrieval. The regional weighted AOT is computed by averaging the AOT of all aerosol mixtures weighted by the inverse of chi-squared statistics. The quality of the MISR AOT in each grid is indicated by reporting the "successful retrieval flag". Following previous studies (Diner et al., 2001), this study uses the regional mean AOT that is the mean AOT of all successful aerosol mixtures and has been shown to contain minimum regional bias and is therefore suitable for intercomparison purposes.

The MISR instrument has a swath width of about 380 km and orbits the Earth with 233 distinct orbits that are repeated every 16 d. Only four different satellite orbit paths could cover the SP site (40.09°N, 94.41°E). In total we obtained 21 $\tau_{\mathrm{MISR}}/\tau_{\mathrm{SP}}$ coincidence pairs that met the comparison criteria over the study period (Table 1). Note that the MISR was launched in December 1999 and started to collect data in February 2000. As shown in Fig. 2a, most $\tau_{\mathrm{SP}}/\tau_{\mathrm{MISR}}$ pairs show a good agreement and generally fall within the expected uncertainties (i.e. maximum of 0.05 or 20% of τ_{MISR}). However, several pairs with large spatial variations (in τ_{MISR}) and temporal variations (in τ_{SP}) have larger differences between τ_{MISR} and τ_{SP}, that result in a low linear correlation coefficient of 0.62 and a large root-mean-square (rms) error value of 0.15.

Table 1. Statistics of collocated MISR data and sunphotometer (SP) data used in this study. In total there are four different satellite orbit paths that could cover the SP site (40.09°N, 94.41°E). For each path, an array of 3 × 3 MISR AOT grids centred at the location of the SP site is used for the comparison with SP AOTs. The latitude and longitude of the centre grid in different paths as well as its distance to the SP site are shown in the following. For each comparison pair, the date (mm/dd/2000), the number of valid MISR AOT points N_v, and the number of SP AOT points within 30 min of the satellite passing time are also shown.

MISR path no	Latitude	Longitude	Distance to SP	Specific information about collocated pairs						
136	40.15°N	94.35°E	8.23 km	Date	03/24	04/09	04/25	06/28	07/14	11/19
				MISR N_v	3	3	2	7	8	2
				SP Points	5	4	4	2	3	6
137	40.15°N	94.47°E	8.23 km	Date	03/15	05/18	06/19	07/21	08/22	09/07
				MISR N_v	5	4	3	6	5	6
				SP points	5	3	3	3	4	5
138	40.16°N	94.38°E	8.23 km	Date	03/22	05/25	07/12	07/28	08/13	08/29
				MISR N_v	5	6	6	5	7	3
				SP points	5	4	3	4	4	5
139	40.12°N	94.5°E	8.23 km	Date	4/30	5/16	6/17			
				MISR N_v	1	2	3			
				SP	5	4	4			

Due to the different viewing geometry between the SP and the MISR, one of the important factors that needs to be considered during the intercomparison is possible cloud contamination in the 3 × 3 MISR regions (Diner et al., 2001). To account for this, we evaluate the number of valid and successful MISR AOT (N_v) in the 3 × 3 regions based on the MISR AOT retrieval successful flag. Diner et al. (2001) performed a similar analysis for all available coincident τ_{SP}/τ_{MISR} pairs as long as N_v is larger than 1. We further evaluate the comparison criteria for different N_v values ranging from 1 to 9 (Table 1). Another factor that must be considered is the quality and the temporal variations of τ_{SP}. Diner et al. (2001) make a quality assessment (QA) status of τ_{SP} based on the standard deviation of τ_{SP} (hereafter σ_{SP}) within ±30 min of the MISR overpass (QA is excellent if $\sigma_{SP} < 0.01$; good if $\sigma_{SP} < 0.02$; fair if $\sigma_{SP} < 0.04$; and questionable if $\sigma_{SP} > 0.04$). This classification system is useful because the total time the MISR takes to image a given location is relatively short (about 7 min) and therefore may not represent the mean state of the atmosphere, especially when AOT has large temporal variations. However, based on the analysis of our SP AOT data, we conclude that the QA criteria reported by Diner et al. (2001) for smoke aerosols may be too stringent for dust aerosols near the desert regions since τ_{SP} could change by about 0.2–0.5 in 1 to 2 h during the passage of a dust front.

By considering daily and hourly τ_{SP}variations, we found that only one collocation pair on 9 April 2000 is questionable. On this day, the τ_{SP} was about 0.2 in the early morning, and increased dramatically to 1.5 and then decreased to about 1.0 in late morning (Fig. 3). The AOT shows large fluctuations on this day, with diurnal change of 1.3, and daily mean value of 0.8 with a standard deviation about 0.3. The four τ_{SP} points that are within ±30 min of MISR overpass have values of 0.79, 0.82, 0.94 and 0.97, with an hourly change of about 0.2. Therefore, this τ_{SP}/τ_{MISR} pair does not meet the quality criteria for the intercomparison and was not used in subsequent analysis. We argue that this exclusion does not necessarily indicate that the quality of τ_{SP} is questionable but merely indicates the differences due to measurement methods.

Figures 2b and c show the τ_{SP}/τ_{MISR} intercomparison for $N_v \geq 1$ and 5 respectively and relevant statistics for different N_v criteria are shown in Table 2. When $N_v = 4$, the statistics of the τ_{SP}/τ_{MISR} comparison become stable and comparisons become better, i.e. the linear correlation coefficient R is larger than 0.9 with a rms error of about 0.05. Although the MISR retrievals are within the expected uncertainties, the MISR tends to overestimate the SP AOT in all cases and when N_v decreases, the over-estimation is generally larger (Table 2). However, for $N_v > 7$, there are only three intercomparison pairs left, hampering the further exploration of the effect of N_v on the change of τ_{MISR} uncertainties. We note that cloud contamination is one possibility that could result in invalid AOT retrievals and hence a decrease in N_v. Other factors, including the non-ideality in the prescribed aerosol models and sharp topographic variations, could also influence the success of the retrievals. Table 2 suggests that there is about a 0.05 systematic over-estimation in the MISR aerosol optical thickness values, even when retrieval conditions are favourable. Although the implication of such an overestimation on the MISR dust retrieval algorithms needs to be further explored, the possible reasons could include non-ideality of dust optical properties such as low single-scattering albedo or instrument calibration uncertainties.

We finally explore whether τ_{MISR} during the time of the satellite overpass is representative of the daily mean dust AOTs near dust source regions. This is important because MISR dust AOT is essentially an instantaneous quantity. Due to the scarcity of AOT information over desert regions, the MISR dust AOT plays an

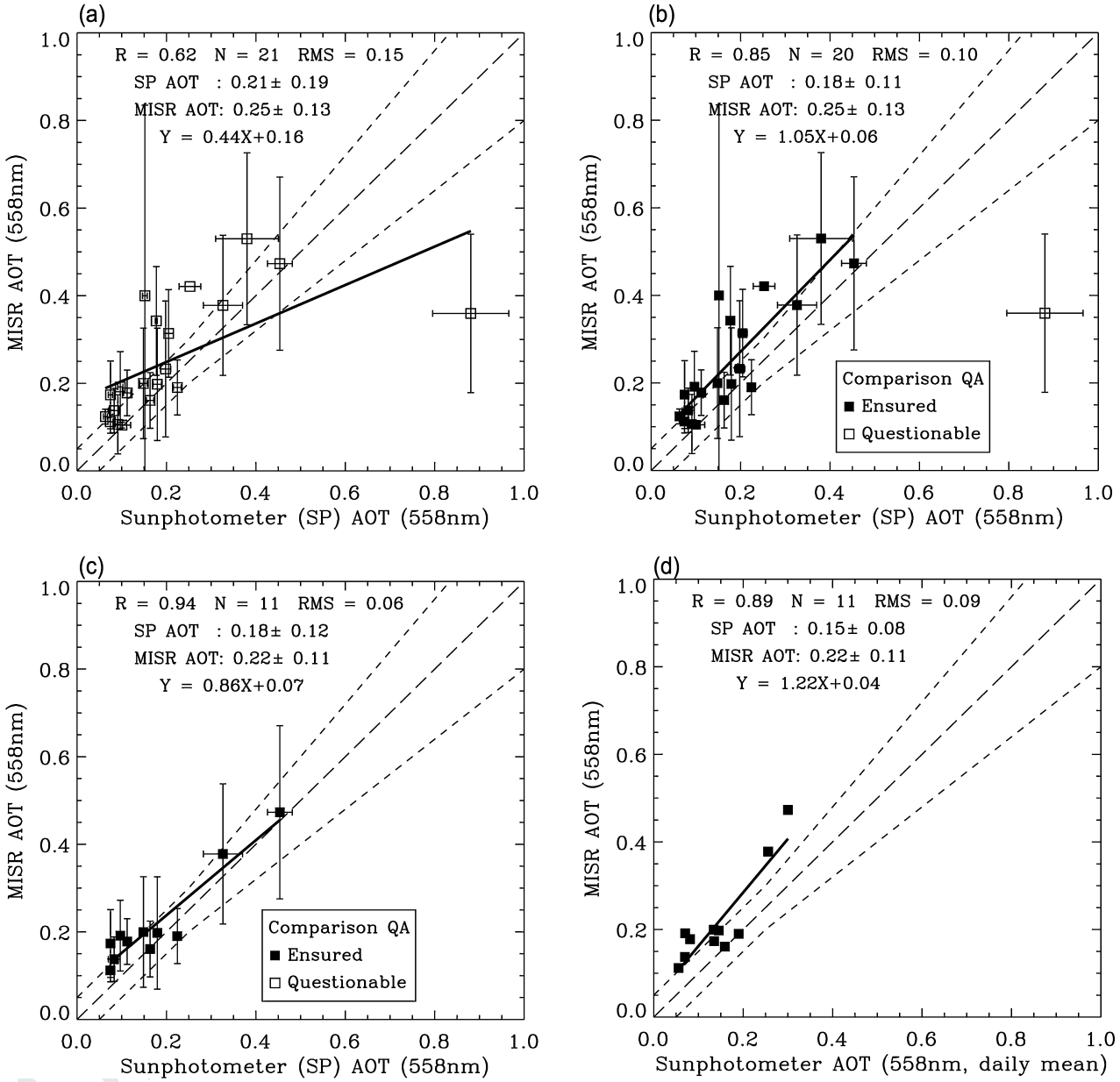

Fig 2. Intercomparison between MISR and sunphotometer AOT for (a) all coincident pairs, (b) all quality-ensured comparison pairs and (c) pairs that have at least five valid MISR AOT values in the 3 × 3 sets regions. (d) Comparison of *daily-mean* sunphotometer AOT and MISR AOTs that have at least five valid MISR AOT values in 3 × 3 set regions. The horizontal bars represent the temporal standard deviations and vertical bars represent the spatial standard deviations. In panel (b) the open diamond represents questionable data. The long-dashed line represents the one-to-one line and the short-dashed line represents the expected MISR AOT uncertainty line (e.g. 0.05 or 20% of MISR AOT, whichever is larger).

important role in dust forcing calculations (Zhang and Christopher 2003) However, the instantaneous values must be converted to diurnally averaged quantities. Therefore, the intent of the intercomparison between τ_{MISR} and daily mean τ_{SP} is not to evaluate the MISR AOT product and retrieval algorithm itself, but rather to investigate possible uncertainties if we use τ_{MISR} as a daily mean value in the radiative forcing calculations over the East Asian desert regions. For $N_{\mathrm{v}} \geq 5$, Fig. 2d shows that τ_{MISR} and the daily mean τ_{SP} are highly correlated ($R = 0.89$); but on the average, the difference between τ_{MISR} and the daily mean SP AOT is about 0.09. Accounting for the current τ_{MISR} instantaneous bias of 0.05, the τ_{MISR} will over-estimate the τ_{SP} by about 0.03 even if the accuracy of τ_{MISR} is improved to within 0.01. The MISR on-board the Terra satellite usually samples the diurnal phase of AOT at 10:45 a.m. local time (Diner et al., 2001). Therefore, the AOT bias of 0.03 is the sampling error

Table 2. Statistics of comparison between MISR AOT (τ_{MISR}) and sunphotometer (SP) AOT (τ_{SP}) using different thresholds (N_{v} defined as the number of valid AOT points in the array of 3 × 3 MISR AOT grids) in cloud-free conditions where N is the number of comparison pairs, R is the linear correlation coefficient, $\bar{u} \pm \sigma$ is the mean and standard deviation, rmse is the root mean square error and ε is the mean bias, defined as mean MISR AOT minus mean of SP AOT.

Threshold N_{v}	N[a]	R	Best fit linear equation	MISR AOT ($\bar{u} \pm \sigma$)	SP AOT ($\bar{u} \pm \sigma$)	Mean bias	rmse
1	20	0.85	$\tau_{\mathrm{MISR}} = 1.05\,\tau_{\mathrm{SP}} + 0.06$	0.25 ± 0.13	0.18 ± 0.11	0.07	0.10
2	19	0.85	$\tau_{\mathrm{MISR}} = 1.01\,\tau_{\mathrm{SP}} + 0.06$	0.24 ± 0.13	0.17 ± 0.11	0.07	0.09
3	16	0.86	$\tau_{\mathrm{MISR}} = 0.97\,\tau_{\mathrm{SP}} + 0.07$	0.25 ± 0.13	0.18 ± 0.11	0.07	0.09
4	12	0.95	$\tau_{\mathrm{MISR}} = 0.85\,\tau_{\mathrm{SP}} + 0.07$	0.21 ± 0.11	0.17 ± 0.12	0.04	0.06
5	11	0.94	$\tau_{\mathrm{MISR}} = 0.86\,\tau_{\mathrm{SP}} + 0.07$	0.22 ± 0.11	0.18 ± 0.12	0.04	0.06
6	7	0.95	$\tau_{\mathrm{MISR}} = 0.81\,\tau_{\mathrm{SP}} + 0.09$	0.25 ± 0.12	0.21 ± 0.14	0.04	0.07
7	3	0.33	$\tau_{\mathrm{MISR}} = 0.04\,\tau_{\mathrm{SP}} + 0.18$	0.19 ± 0.01	0.14 ± 0.07	0.05	0.07
8	1	–	–	0.19 ± 0.06	0.22 ± 0.01	−0.03	0.03

[a]One pair with the questionable quality assessment of SP AOT on 9 April 2000 is not considered in this comparison (see text). Hence, a total of 20 out of 21 pairs in Table 2 are used in the comparison with different threshold tests. The questionable pair is filtered out when the threshold larger is than 3. There are no intercomparison pairs left when the threshold value is 9.

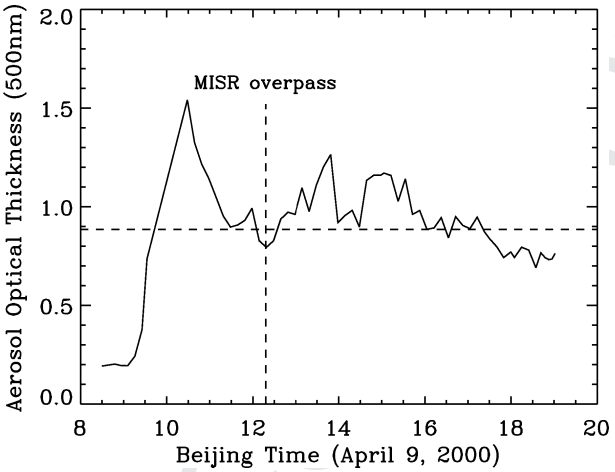

Fig 3. Diurnal variation of dust AOT on 9 April 2000. The horizontal dashed line shows the daily mean AOT.

mainly caused by the diurnal variation of dust in its source regions and cannot be resolved by the refinement of MISR retrieval algorithms alone. Consistent with this study, Wang et al. (2004) also showed that the diurnal variations of dust AOT and dust Q1 Angstrom exponent at the Dunhuang observation site is larger than 10%, and 30% respectively.

Although the diurnal variations of AOT near dust source regions may be less important for climate studies that average over large spatial and temporal domains, they are important for regional studies that examine radiative forcing, air quality and other numerical modelling studies. Using a delta-four stream radiative model (Fu and Liou, 1993) modified for dust radiative forcing studies (Christopher et al., 2003), we estimate the effect of a 10% diurnal variation of dust AOT on the radiative forcing at the top of atmosphere and the surface. For a daily mean AOT of 0.3 (at 0.55 μm) in Dunhuang, a 10% variation of AOT will generally result in 5–8% change of TOA forcing, and 8–12% of forcing at the surface, though the specific values will depend on the diurnal pattern assumed in the model. Therefore for regional studies that require a more accurate representation of the diurnal variability of aerosol optical thickness in dust source regions, caution must be exercised when interpolating the AOT from polar-orbiting sensors into the time-averaged forcing calculations. The current and future generation of geostationary satellites (Schmetz et al., 2002) could play a vital and complementary role to the polar-orbiting satellites to further enhance our understanding of dust aerosols.

4. Conclusion

We conclude that the agreement between τ_{MISR} and τ_{SP} improves when retrieval conditions such as cloud cover, topography and aerosol properties are favourable. Although τ_{MISR} are highly correlated with τ_{SP}($R > 0.9$) and fall within the predicted uncertainties (0.05 or 20% of τ_{SP}, whichever is larger), they over-estimate the τ_{SP} by about 0.05 in the current version of MISR aerosol product (F06_0013). The τ_{MISR} seems to have larger biases during the pass of heavy dust storms when dust optical properties might have high temporal variations. There is an additional bias of about 0.03 between the instantaneous values of τ_{SP} at the MISR overpassing time and its daily mean. Therefore, the diurnal change of dust AOT and other dust optical properties needs to be carefully treated in the current estimation of aerosol forcing studies, especially if τ_{MISR} is used to represent the daily mean AOT near dust source regions.

5. Acknowledgments

This research is supported by NASA's Radiation Sciences, Interdisciplinary Sciences and ACMAP programs. We thank Dr

Xiang-Ao Xia in the Institute of Atmospheric Physics (IAP), Chinese Academy of Sciences (CAS) for providing the sunphotometer data. We thank Dr Ralph Kahn for his encouragement in writing this manuscript, and an anonymous reviewer for a critical review and helpful suggestions that improved the quality of this paper.

References

Christopher, S. A., Wang, J., Ji, Q. and Tsay, S.-C. 2003. Estimation of shortwave dust aerosol radiative forcing during PRIDE. *J. Geophys. Res.* **108**, doi:10.1029/2002JD002787.

Diner, D. J., Abdou, W. A., Bruegge, C. J., Conel, J. E., Crean, K. A. et al. 2001. MISR aerosol optical depth retrieval over southern Africa during the SAFARI-2000 season campaign. *J. Geophys. Lett.* **28**, 3127–3130.

Eck, T. F., Holben, B. N., Reid, J. S., Dubovik, O., Smirnov, A. et al. 1999. Wavelength dependence of the optical depth of biomass burning, urban, and desert dust aerosols. *J. Geophys. Res.* **104**, 31 333–31 349.

Fu, Q. and Liou, K. N. 1993. Parameterization of the radiative properties of cirrus clouds. *J. Atmos. Sci.* **50**, 2008–2025.

Hansen, J., Sato, M. and Ruedy, R. 1997. Radiative forcing and climate response. *J. Geophys. Res.* **102**, 6831–6864.

Harrison, L. and Michalsky, J. 1994. Objective algorithms for the retrieval of optical depths from ground-based measurements. *Appl. Opt.* **33**, 5126–5132.

Holben, B. N., Tanré, D., Smirnov, A., Eck, T. F., Slutsker, I. et al. 2001. An emerging ground-based aerosol climatology: Aerosol optical depth from AERONET. *J. Geophys. Res.* **106**, 12 067–12 097.

Husar, R. B. T., Schichtel, D. M., Falke, B. A., Li, S. R., Jaffe, F. et al. 2001. Asian dust events of April 1998. *J. Geophys. Res.* **106**, 18 317–18 330.

IPCC, Climate Change 2001. *The Scientific Basis: Contribution of Working Group I to the Third Assessment Report of the Intergovernmental Panel on Climate Change* (eds) J. T. Houghton, Y. Ding, D. J. Griggs, M. Noguer, P. J. van der Linden (et al.), Cambridge University Press, Cambridge.

Kahn, R., Banerjee, P., McDonald, D. and Martonchik, J. 2001. Aerosol properties derived from aircraft multiangle imaging over Monterey Bay. *J. Geophys. Res.* **106**, 11 977–11 995.

Kaufman, Y. J., Tanre, D. and Boucher, O. 2002. A satellite view of aerosols in climate systems. *Nature* **419**, 215–223.

Martonchik, J. V., Diner, D. J., Crean, K. A. and Bull, M. A. 2002. Regional aerosol retrieval results from MISR. *IEEE Trans. Geosci. Remote Sensing* **40**, 1520–1531.

Martonchik, J. V., Diner, D. J., Kahn, R. A., Ackerman, T. P., Verstraete, M. M. et al. 1998. Techniques for the retrieval of aerosol properties over land and ocean using multiangle imaging. *IEEE Trans. Geosci. Remote Sensing* **36**, 1212–1227.

Nakajima, T., Tonna, G., Rao, R., Boi, P., Kaufman, Y. and Holben, B. 1996. Use of sky brightness measurements from ground for remote sensing of particulate polydispersions. *Appl. Opt.* **35**, 2672–2686.

Remer, L. A., Tanré, D., Kaufman, Y. J., Ichoku, C., Mattoo, S. et al. 2002. Validation of MODIS aerosol retrieval over ocean. *Geophys. Res. Lett.* **29**, doi:10.1029/2001GL013204.

Schmetz, J., Pili, P., Tjemkes, S., Just, D., Kerkmann, J. et al. 2002. An introduction to METEOSAT Second Generation (MSG). *Bull. Am. Meteorol. Soc.* **81**, 977–1001.

Smirnov, A., Holben, B. N., Eck, T. F., Dubovik, O. and Slutsker, I. 2000. Cloud screening and quality control algorithms for the AERONET data base. *Remote Sensing Environ.* **73**, 73 337–73 349.

Tanré, D., Haywood, J., Pelon, J., Léon, J. F., Chatenet, B. et al. 2003. Measurement and modeling of the Saharan dust radiative impact: overview of the Saharan Dust Experiment (SHADE). *J. Geophys. Res.* **108**(8547), doi:10.1029/2002JD003273.

Wang, J., Christopher, S. A., Reid, J. S., Maring, H., Savoie, D. et al. 2003a. GOES 8 retrieval of dust aerosol optical thickness over the Atlantic Ocean during PRIDE. *J. Geophys. Res.* **108**, doi:10.1029/2002JD002494.

Wang, J., Liu, X., Christopher, S. A., Reid, J. S., Reid, E. A. et al. 2003b. The effects of non-sphericity on geostationary satellite retrievals of dust aerosols. *Geophys. Res. Lett.* **30**, doi:10.029/2003GL018697.

Wang, J., Xia, X., Wang, P. and Christopher, S. A. 2004. Diurnal variability of dust aerosol optical thickness and angstrom exponent over dust source regions in China. *Geophys. Res. Lett.* **31**(8), doi:10.1029/2004GL019580.

Zhang, J. and Christopher, S. A. 2003. Longwave radiative forcing of dust aerosols over the Saharan Desert estimated from MODIS, MISR, and CERES observations from Terra. *Geophys. Res. Lett.* **30**, doi:10.1029/2003GL018479.

Zhao, T. X.-P., Stowe, L. L., Smirnov, A., Crosby, D., Sapper, J. et al. 2002. Development of global validation package for satellite oceanic aerosol optical thickness retrieval based on AERONET observations and its application to NOAA/NESDIS operational aerosol retrievals. *J. Atmos. Sci.* **59**, 294–312.